SCIENTIFIC REPORTS

OPEN

SUBJECT AREAS:
CELLULAR MICROBIOLOGY
ENVIRONMENTAL MICROBIOLOGY
BIOPHYSICS
BACTERIAL STRUCTURAL BIOLOGY

Received
12 July 2012

Accepted
12 October 2012

Published
10 December 2012

Correspondence and requests for materials should be addressed to L-FW. (wu@imm.cnrs.fr)

* These authors contributed equally to this work.

† Current address: Institut Curie, UMR 144 CNRS, Cell and Tissue Imaging Facility (IBiSA), F-75248, Paris, France

Structural properties of the tubular appendage spinae from marine bacterium *Roseobacter* sp. strain YSCB

A. Bernadac[1]*, L.-F. Wu[2,8]*, C.-L. Santini[2,8], C. Vidaud[3], J. N. Sturgis[4], N. Menguy[5,8], P. Bergam[1†], C. Nicoletti[6] & T. Xiao[7,8]

[1]Service de Microscopie Electronique, [2]Laboratoire de Chimie Bactérienne, UMR 7283; Institut de Microbiologie de la Méditerranée, Aix-Marseille University, CNRS, 31 chemin Joseph Aiguier, 13402 Marseille cedex 20, France, [3]Laboratory of target protein studies, Institut de Biologie Environnementale et de Biotechnologie, CEA Marcoule, BP 17171, F-30207 Bagnols-sur-Cèze, France, [4]Laboratoire d'Ingénierie des Systèmes Macromoléculaires UMR 7255, Institut de Microbiologie de la Méditerranée, Aix-Marseille University, CNRS, 31 chemin Joseph Aiguier, 13402 Marseille cedex 20, France, [5]IMPMC, UMR 7590 CNRS, Université Pierre et Marie Curie, IPGP, IRD, Case courrier 115, 4 Place Jussieu, 75252 Paris Cedex 05, France, [6]Aix Marseille Université, CNRS, ISM2, UMR-7313, 13397, Marseille cedex 20, France, [7]Key Laboratory of Marine Ecology & Environmental Sciences, Institute of Oceanology, Chinese Academy of Sciences, Qingdao 266071, China, [8]Laboratoire International Associé de la Bio-Minéralisation et Nano-Structures (LIA-BioMNSL), CNRS, F-13402 Marseille cedex 20, France.

Spinae are tubular surface appendages broadly found in Gram-negative bacteria. Little is known about their architecture, function or origin. Here, we report structural characterization of the spinae from marine bacteria *Roseobacter* sp. YSCB. Electron cryo-tomography revealed that a single filament winds into a hollow flared base with progressive change to a cylinder. Proteinase K unwound the spinae into proteolysis-resistant filaments. Thermal treatment ripped the spinae into ribbons that were melted with prolonged heating. Circular dichroism spectroscopy revealed a dominant beta-structure of the spinae. Differential scanning calorimetry analyses showed three endothermic transformations at 50–85°C, 98°C and 123°C, respectively. The heating almost completely disintegrated the spinae, abolished the 98°C transition and destroyed the beta-structure. Infrared spectroscopy identified the amide I spectrum maximum at a position similar to that of amyloid fibrils. Therefore, the spinae distinguish from other bacterial appendages, e.g. flagella and stalks, in both the structure and mechanism of assembly.

The *Roseobacter* clade is one of the major groups of marine *Proteobacteria*[1]. They are broadly distributed across diverse marine environments from coastal to open oceans and from sea ice to sea floor. The members of this clade share >89% identity of the 16S rRNA genes[1]. The *Roseobacter* clade are physiologically very versatile and play an important role in global marine biogeochemical cycles. They are often associated with organic or inorganic surfaces and their association with larvae or alga may serve as probiotics to protect these organisms against pathogenic bacteria[2–6]. Various surface appendages including flagella, pili and holdfast have been observed for *Roseobacter* and play an important role in the surface adhesion and colonization of this clade of microorganisms[7]. However, spinae have not been observed for *Roseobacter* clade despite their wide distribution in both marine and freshwater bacteria.

Spinae are hollow, tubular appendages with transverse striation and are distinct from flagella, pili and stalks. Spinae were first observed for *Agrobacterium* sp. by Moll and Ahrens in 1970[8], then have been found in wide arrange of bacteria including strain marine pseudomonad D71[9], *Chlorobium* spp.[10,11], *Desulforhopalus singaporensis*[12], *Methylocystis echinoides*[13] and *Cyanobium* sp. with up to hundreds spinae per cell[14]. There is species specificity in the morphology of the spinae. They vary in length and in width, and some have a conical base whereas others taper to the distal tip. The function of spinae has not been experimentally demonstrated although various roles have been hypothesized, such as buoyancy to maintain the cells in aquatic habitat[15], promotion of cellular aggregation[14] and signal exchange between cells[16]. The most extensively characterized spinae are those from the strain marine pseudomonad D71[9,17,18] that was renamed as *Spinomonas maritima*[16]. They are proposed to consist of a 42 kDa spinin-specific protein with an estimated content of about 2.5×10^5

spinin molecules per cell, which constitutes a substantial portion of the total protein of a spinae-producing bacterium[17,19].

Recently, we have isolated a novel member of the *Roseobacter* clade from the Yellow Sea, China[20]. Phylogenetic analysis of the 16S rRNA gene sequences reveals that the new isolates (YSCB1, YSCB2, YSCB3 and YSCB4) are identical to uncultured Arctic seawater bacterium R7967 (99.57–100% sequence identity) and closely related to the cultured *Roseobacter* sp. DSS-1 (99.27–99.76% sequence identity) isolated from the southeastern coastal water of the USA. YSCB strains possess intracellular chromium-containing aggregates. Therefore, they exhibit a peculiar property in mineral biogeneration compared to other members of the *Roseobacter* clade. In addition, spinae were occasionally observed on these strains. Here we report characterization of spinae structure of the YSCB strains. Using biochemistry, biophysics and microscopy analyses we found that the spinae of *Roseobacter* sp. YSCB strains are built from proteolysis-resistant filaments winding into a tubular architecture. The spinae are either unwound into the filaments by proteinase-catalyzed proteolysis or unripped into ribbons when heated. Therefore, the spinae seem to be built up by a mechanism different from those of other bacterial appendages.

Results

Production of spinae by *Roseobacter* sp. isolates. The *Roseobacter* YSCB isolates are heterotrophic, marine bacteria that have been isolated from the Yellow Sea Cold Water Mass at 70 m depth[20]. They showed different colony morphology, smooth for YSCB-1 and YSCB-3 and rough for YSCB-2 and YSCB-4, when they were initially isolated on Marine Broth 2216 plates. Because their 16S rRNA gene sequences are virtually identical, and they show the same features for all genetic and physiological analyses and they can all change colony phenotypes depending on the growth phase and conditions, we consider the four isolates as the same species and thus refer to them as *Roseobacter* sp. strains. The results described here are common to all four isolates and will not be reported for individual strains. Transmission electron microscopy (TEM) observation rarely reveals a single flagellum at one pole of some cells (Supplementary information, Figure S1, A). Consistently, we observed that less than one percent of cells in a population could swim smoothly, but most of them showed a non-directional movement, probably as a result of both inefficient flagellar propulsion and Brownian motion.

The cells were routinely grown in Marine Broth 2216 media. Occasionally, surface appendages, referred to as spinae, were observed on a few cells (Supplementary information, Figure S1, B). Despite the fact that flagella are observed for most *Roseobacter* spp.[7], the spine-like extracellular appendage has not previously been reported for the members of this clade.

We sought to optimize growth conditions for the production of the spinae. Temperatures, shaking speed as well as the pH of the media increase neither the number of spinae on a cell nor the proportion of population with spinae. Spinae were almost absent from the cells grown on plates. Finally, we found that dilution of the Marine Broth 2216 liquid media to half strength drastically increased the production of the spinae but had no effect on flagellar production. Under these conditions, almost all cells have spinae (Fig. 1, A). The number of spinae was maximal in the stationary phase. Each cell might have a dozen of spinae up to 3 μm in length and resemble a long-spined sea urchin (Fig. 1, A). Further dilution of Marine Broth media slowed down bacterial growth without increasing the spine production. In contrast, increasing NaCl concentration in the diluted media progressively decreased spine production. Under all growth conditions, the spinae appeared after 2-day incubation and reached maximal number at the stationary growth phase after 4–5 day incubation. Therefore, the kinetics of spinae synthesis does not seem to be affected by the growth media.

The spinae were distributed randomly on the cellular surface when analyzed by transmission electron microscopy (TEM) and cryo-electron microscopy (cryo-EM). Scars appeared at the places where spinae were mechanically detached from a cell (Fig. 1, B). The scars seemed to be closed without the leak of the cytosol. Moreover, no internal sub-structure like the flagellar basal body was observed on the cryo-EM images (Fig. 1, C). This finding suggests that the spinae are unlikely to be a rotary apparatus and probably assembled through a mechanism different from that of the flagella. The overall morphology of the spinae resembles the Eiffel Tower, consisting of a flared base connected to a columnar or tubular structure with transverse ribs. Therefore, we also call them Eiffel Towers.

A literature search revealed that the spinae are similar to those of the strain marine pseudomonad D71[9]. Although the taxonomic name *Spinomonas maritima* has been proposed to the strain marine pseudomonad D71[16], we do not know how closely related are *Roseobacter* sp. YSCBs and marine pseudomonad D71 because of the absence of molecular genetic data, i.e. 16S rRNA gene sequence of the D71 strain. Notably, *Roseobacter* sp. YSCBs have almost no spinae when incubated in the growth media optimized for the spinae production for the strain marine pseudomonad D71[16] (data not shown). Either these two strains belong to different species or one carries a regulatory mutation affecting the spine synthesis.

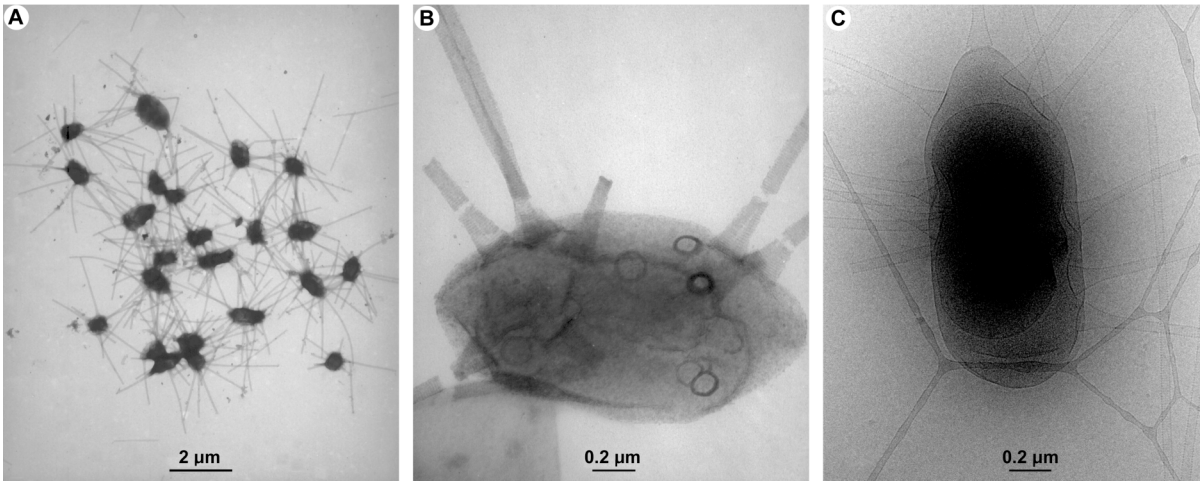

Figure 1 | Distribution of spinae on *Roseobacter* sp. YSCB cells. Negatively stained (1% uranyl acetate) TEM micrographs (A and B) and non-stained cryo-EM micrograph (C) showed the random distribution of spinae and the scars after mechanical removal of spinae (B).

Microscopy characteristics of the spinae of the *Roseobacter* sp. strains. To characterize the physico-chemical property of the spinae we have purified the spinae. After analyses with various buffers, we found that the spinae are extremely stable in water. The final protocol used for purification of the spinae consists of washing and resuspending the harvested cells with deionized water, then mechanically shearing to detach the spinae and collecting them by centrifugation (see Methods for details). Inspection by transmission electron microscopy showed highly purified, intact spinae (Fig. 2, A1). Flagella with a diameter of about 18 nm were sometimes found in the samples (arrowhead in Fig. 3, B). Amplified view of the tubular part showed obvious helical structure (Fig. 2, A2). We further analyzed the fine structure of the spinae with various microscopy techniques. Atomic force microscopy (AFM) confirmed the feature of cylinder with flared base and the shallow pitch (Fig. 2, B1 and B2). Cryo-EM preserved structures in their native state and without staining provided more and finer details (Fig. 2, C1 to C4, on line movie). The spinae are composed of a flared base with the enlarged side attached on the surface of the cells and a tubular part connected on the narrow side of the base. Clearly, the spinae are not extension of the cell wall. Based on about 100 measurements, we found that the size of the flared bases is 139.2 ± 10.2 nm (mean ± standard deviation) for the enlarged side, 46.5 ± 3.9 nm for the narrow side and 137.4 ± 3.8 nm for the height. The cylindrical part has a width similar to the narrow end of the base and a variable length probably exacerbated by breakage during sample preparation. The helical pitch is 11.6 ± 1.0 nm per turn and a striation has an inclination of 6.6 ± 0.8° to the short axis. Reconstitution of the spinae structure from the sections of cryo-tomographs showed clearly that a single filament winds to form the left-handed helical flared base that progressively transforms into the cylinder (Online movie). The spinae appeared to be hollow from the base to the tip (Fig. 2, C3 and C4).

Biochemical analysis of the spinae. To determine the chemical nature of the spinae, we have treated the purified spinae with trypsin (at final concentration of 1 mg/ml), proteinase K (1 mg/ml), DNase (1 mg/ml), RNase (1 mg/ml), lysozyme (1 mg/ml),

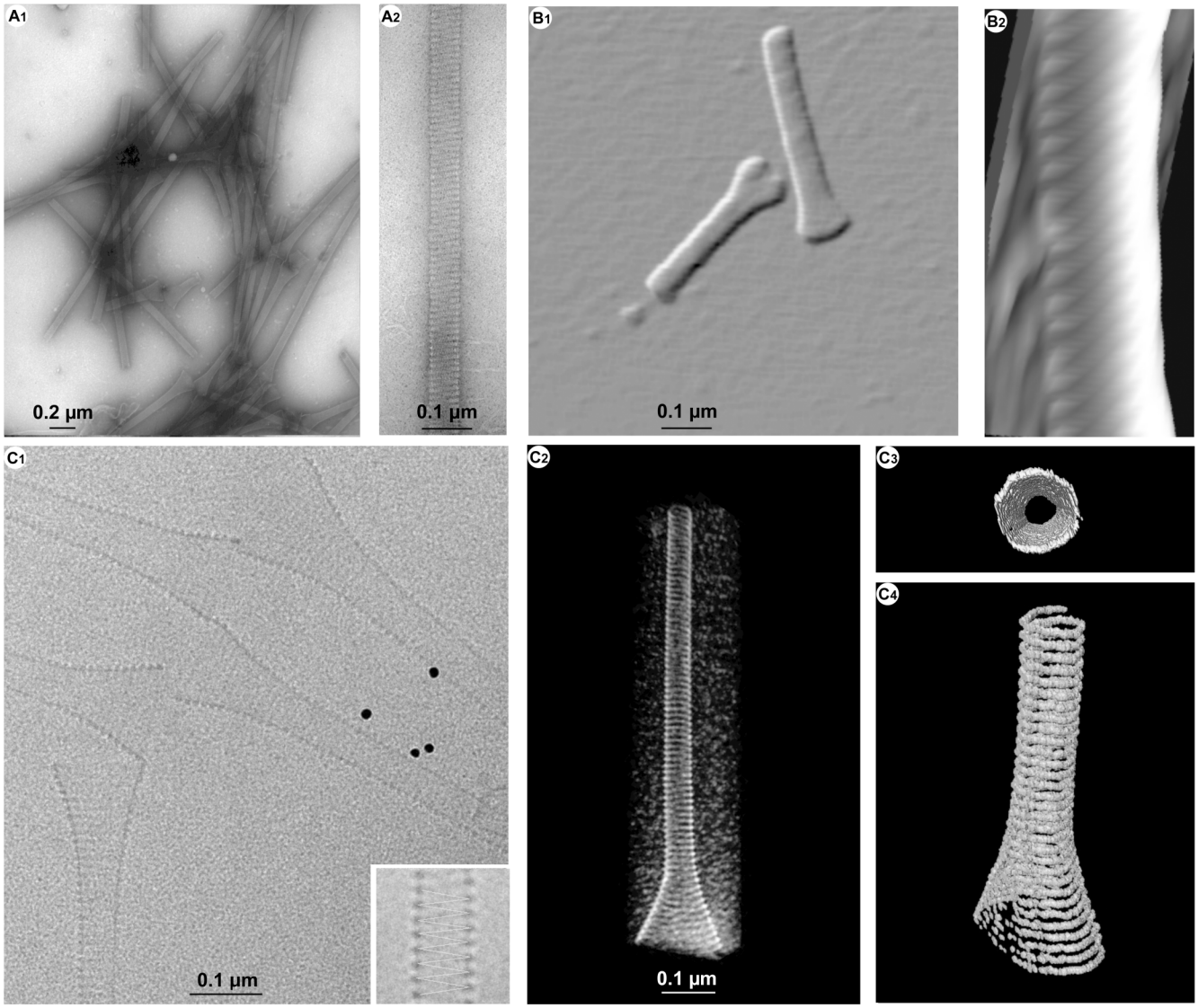

Figure 2 | Structure of *Roseobacter* sp. YSCB spinae. Purified spinae were examined with TEM (A, negatively stained), AFM (B) and cryo-EM (C). The panel A2 is a magnified area of A1 to show the helical structure of the spinae. B2 is dZ/dx derivative view of a segment of B1. The beads (10 nm) in C1 are used for reconstitution of spinae structure from section of cryo-tomographs and the insert in C1 is a magnified view of the helical structure. C2, C3 and C4 show the 3D representation of a tomogram. C2 is a Voltex view and C3 and C4 are segmentations of the tube from bottom to top (without the flared base) and the filament winding of spinae, respectively.

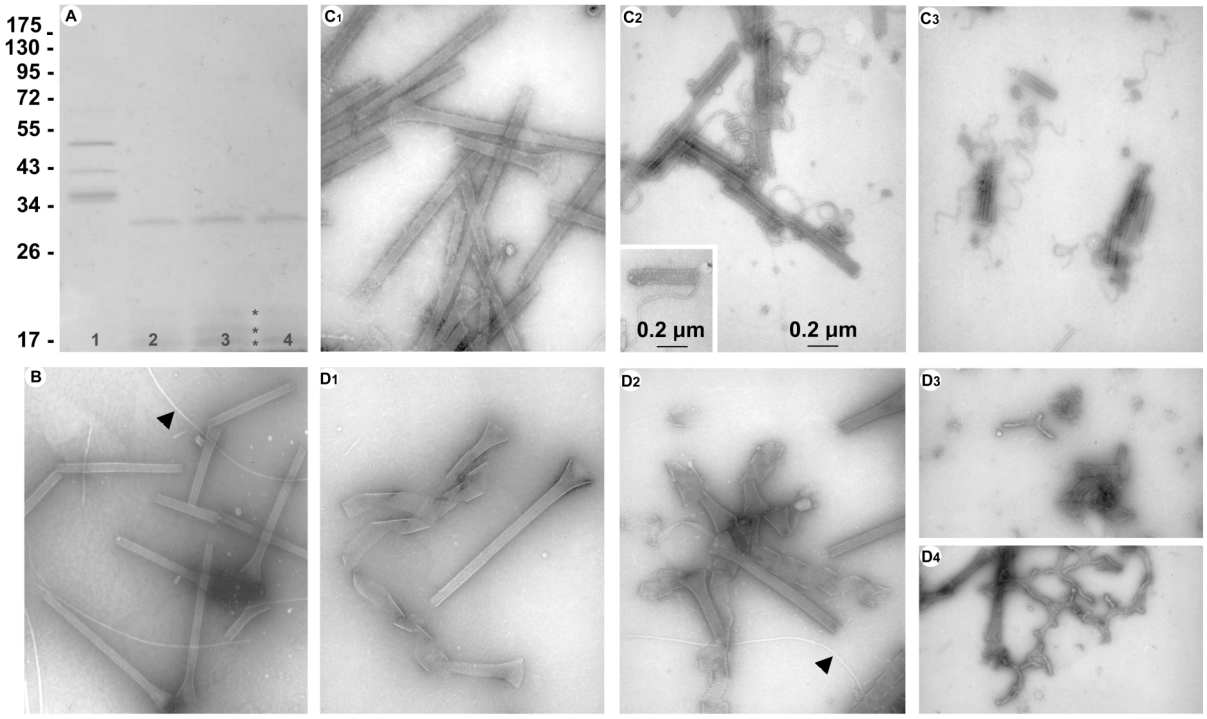

Figure 3 | Disintegration of *Roseobacter* sp. YSCB spinae upon proteolysis or thermal treatments. Purified spinae were examined with SDS-PAGE on 12.5% gels (A, sizes of protein markers on left) or by TEM (negatively stained) without treatment (A, lane 1 and B), or digested with proteinase K at a concentration of 2 mg/ml (A, lane 2; C1), 10 mg/ml (A, lane 3; C2) and 20 mg/ml (A, lane 4; C3), or heated at 100°C for 1 min (D1), 5 min (D2), 10 min (D3 and D4). Insert in C2 shows a single filament winding into the tubular structure. The arrow in B indicates flagellar filament. Asterisks in panel A indicate proteolysis products.

cutinase (45 μg/ml) and DTT (100 mM) and examined the effect by TEM. Under the conditions used, none of these treatments seemed to affect the structural integrity of the spinae (data not shown). These results are consistent with the reported unusual stability of the spinae from the freshwater *Chlorobium* sp. with respect to thermal, chemical and enzymatic treatments[21]. In addition, the spinae from both marine pseudomonad D71 and *Chlorobium* sp. strain JSB1 are resistant to proteases[17,21]. Despite the apparent proteolysis-resistance, it was reported that the spinae of the marine pseudomonad D71 are composed of a single subunit protein, spinin[17,19]. Therefore, we re-assessed the susceptibility of the spinae from *Roseobacter* sp. YSCBs to the proteolysis. We found 4 polypeptides with apparent molecular masses of 68, 50, 42 and 36 (a doublet) kDa (Fig. 3, A) when the purified spinae were resolved by denaturing polyacrylamide gel electrophoresis (SDS-PAGE, see Methods). We intended to identify proteins present in these polypeptide bands by N-terminal sequencing. A sequence of Gln-Ser-Val-Leu-Glu-Arg-Val-Leu was detected for the 36 kDa polypeptide, but only ambiguous short sequences were found in other polypeptides (Fig. S2, Supplementary Information). Searching in the databanks showed that the N-terminal sequence of 36 kDa protein was homologous mainly with hypothetic proteins or some ATPase (Fig. S2, Supplementary Information). To assess if these proteins were the major component of the spinae, we treated the purified spinae with proteinase K at increased concentration compared to the earlier digestion assays. The four polypeptides were completely digested at 2 mg/ml (Fig. 3, A, lane 2 versus lane 1). The 29 kDa bands in lanes 2, 3 and 4 are the added recombinant proteinase K and the polypeptides below are proteolysis products (Asterisks in Fig. 3, A). Notably, the structural integrity of the spinae was preserved when treated with 2 mg/ml proteinase K although the peptides presented in the same samples were completely digested (Fig. 3, A, lane 2; C1 versus B). Therefore, the spinae are probably not assembled from these polypeptides. Interestingly, the spinae structure was unwound into flexible filaments with higher concentration of proteinase K (Fig. 3, C2 and C3). The unwinding might start from the flared base because the base disappeared completely in most micrographs. In addition, we observed that the spinae were unwound in multiple places; pieces of spinae were connected by filaments when the proteinase K concentration was increased to 10 mg/ml or 20 mg/ml (Fig. 3, C2 and C3). In consistence with the results of cryo-tomography reconstitution, each spine seemed to be constructed from a single filament of 9 nm (insert of Fig. 3, C2) that was about half the diameter of the flagella. These results would suggest that the proteolysis-resistant filaments wind into the tubular spinae that is structurally maintained by proteins. Moreover, when whole cells were treated by proteinase K, spinae were detached from the cells without leaving the scars on the cellular surface as observed in the case of mechanical shearing of the spinae (Supplementary information, Fig. S1, D). Therefore, spinae are likely connected to the cellular surface by proteins. Together with cryo-EM analyses, it confirms that the spinae are unlikely to be an extension of the cell wall.

Among other assays for disintegrating the spinae, thermal treatment lead to an intriguing result that is completely different from that of the proteolysis. After 1 min incubation at 100°C, some tubular spinae appeared to be ripped into ribbon (Fig. 3, D1 versus to B). Most spinae were opened after 5 min treatment (Fig. 3, D2) and the rip seemed to initiate from the tip toward to the flared base. After 20 min of treatment, almost all spinae were cut into pieces and even appeared as melted (Fig. 3, D4). These results are different from the reported unusual heat resistance of the spinae of the *Chlorobium* sp., which remain intact after the harsh treatments of autoclave[21]. These findings suggest that spinae from different bacterial species might consist of polymers with different properties.

Biophysical characterization of the spinae. The elemental composition of the spinae was analyzed by X-ray energy dispersive spectroscopy (XEDS). As shown in Fig. 4, A1, the analyzed area

contains virtually only spinae. The salient feature of the XEDS spectrum is that the nitrogen and oxygen were roughly estimated at a ratio less than 1 : 5 that is much lower than the estimated N:O ratio in spinin. Easterbrook and Coombs have reported elemental composition and amino acids distribution of the spinin of marine pseudomonad D71[17]. Based on these data, the calculated N:O ratios are 0.51 and 0.59, respectively. In addition, we calculated, based on the data from the same report, the N:O ratios for flagellin (0.64) and

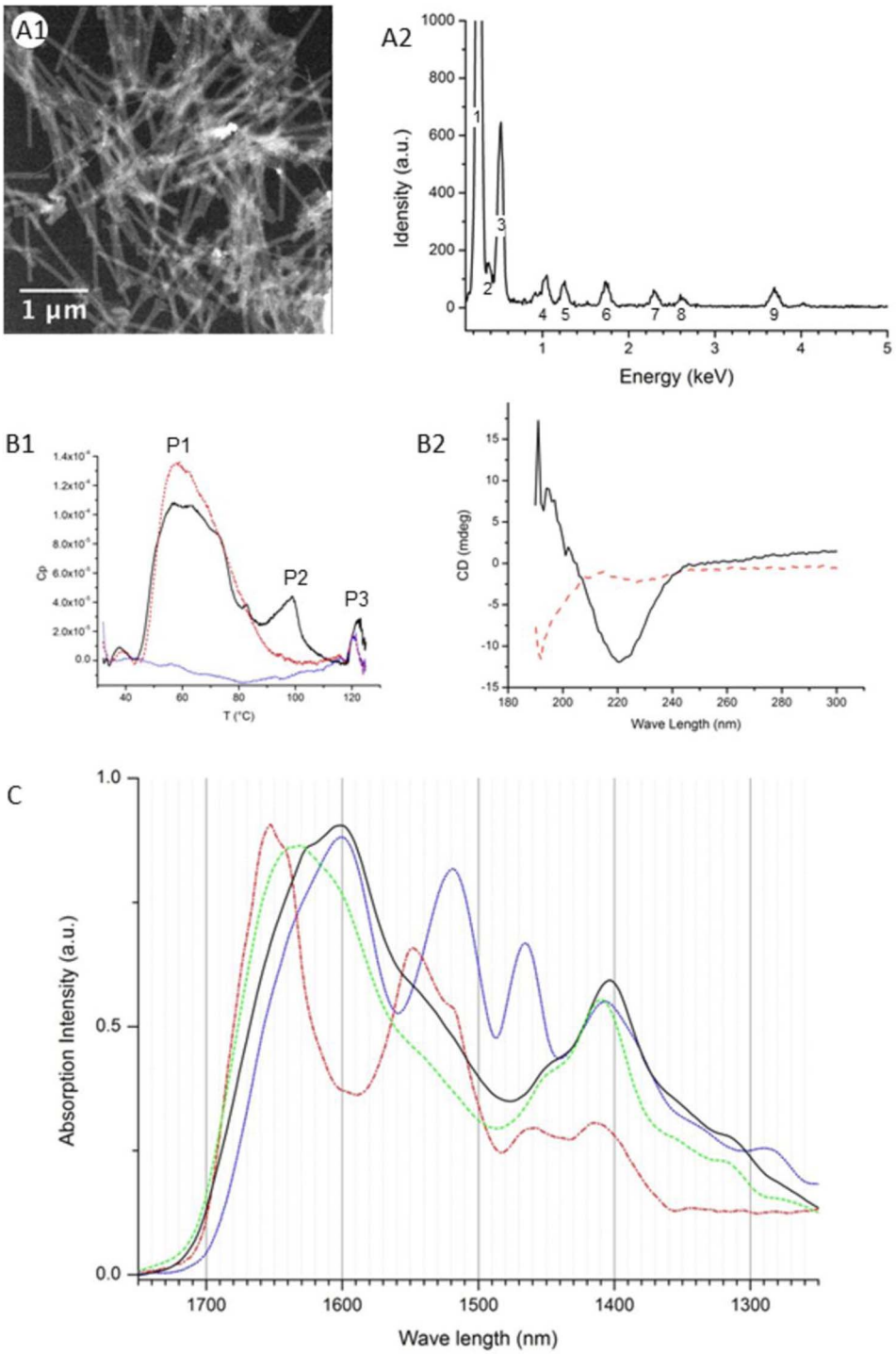

Figure 4 | Biophysical characterization of *Roseobacter* sp. YSCB spinae. Panel A1 (TEM) shows the sample from where the XEDS spectra (A2) were obtained. The peaks correspond to carbon (1), nitrogen (2), oxygen (3), sodium (4), magnesium (5), silicium (6), sulfur (7), chore (8) and calcium (9). Panel B1 is a representative DSC spectrum of the extracted spinae samples. The scan rate is 1°C per min. The thermograms of the subsequent first, second and sixth scan are presented in black (line), red (dash-line) and blue (dot-line), respectively. Panel B2 shows the CD spectroscopy results of the sample before (black line) or after (red dash-line) the first DSC scan. Panel C is IR spectra of amide I bands of the spinae extraction without treatment (black line), or treated at 100°C for 20 min (green dash-line) or with 2 mg/ml proteinase K for overnight at room temperature (blue dot-line). The spectrum of the recombined proteinase K (100 mg/ml) was measured and presented as a reference (red dash-dot-line). The curves are normalized to fit into the same scale.

pilin (0.66). As the XEDS technique used here is only qualitative, further quantitative analysis is required to verify if the main components of the spinae is different from those of the spinin, flagellin and pilins of marine pseudomonad D71. We have used Periodic acid-Schiff staining and lectin binding to assess biochemical nature of the spinae. The results obtained from these assays did not show the presence of carbohydrates (Fig. S3).

The disintegration analyses of the spinae show that proteins maintain the proteolysis-resistant filament winding into the tubular structure. In addition, thermal treatment at 100°C ripped the tubular spinae into ribbons that were melted under prolonged heating. In order to get more information about the chemical and structural nature of the spinae we performed differential scanning calorimetry (DSC) analysis. This technique measures heat flows in or out from a sample that undergoes a physical transformation such as protein denaturing and aggregation or polymer phase transition. While it is generally dedicated to purified macromolecules and at a defined concentration, DSC analyses could provide important qualitative information about the thermal behavior of the components in the extracted spinae fractions. Changes of particle sizes and the secondary structures of the spinae sample before and after the first DSC scan were also monitored with dynamic light scattering (DLS) and circular dichroism (CD). Before the DSC experiment, the samples were composed of two major groups of particles with hydrodynamic diameters of 231.2 nm and 5323 nm. Heating scans were then performed between 30°C and 125°C at 1°C per minute scan rate. No exothermic process was observed in all analysis, showing the absence of strong aggregation of the samples upon the heating[22]. This was further confirmed by the fact that the samples did not present any precipitation or turbidity after each scan, which indicated a thermal stability within this temperature range. Thus the reversibility of the events could be evaluated, and a sample was subjected to up to six subsequent scans at the identical scan rate. As shown in Figure 4, B1, the typical DSC thermogram of the first scan (black curve) displays a very complex melting profile with three major endothermic transitions corresponding to the three major melting peaks P1, P2 and P3. The first one (P1) shows a large irregular and complex shape with many broad transitions, and displays a maximum around 57°C. This feature could be attributed to multi-domain protein or macromolecule unfolding-denaturation, or multiple protein denaturation as generally observed[23–25]. The absorption of heat at 98°C (P2) could be due to the unfolding of a more thermally resistant macromolecule as well as the requirement of heat to rip the tubular spinae as observed with TEM. Interestingly, thermal melting of amyloid fibrils occurs at this temperature region[26]. The small absorption peak at 123°C (P3) was absent from the control-scan with only water as a sample, but was repeatedly observed when the spinae extraction samples were analyzed. After the first DSC scan, DLS results demonstrated a poly-dispersity of the population. The major group of particles was split into two groups of 134.8 nm and 800.9 nm (data not shown). The minor group displayed only a small size shift to 4920 nm with a tiny increase of intensity, which falls into the normal fluctuation region observed in such analysis. The physical change of the sample was further analyzed with circular dichroism spectroscopy. Before heating, the spinae extraction fractions contained macromolecules with essentially beta-sheet structures that were completely destroyed after the heating scan (Fig. 4, B2). Transmission electron microscopy analysis revealed that only trace amount of the spinae was observed, indicating that spinae were virtually completely destroyed by the thermal treatment including a period of 25 min for increasing the temperature from 100°C to 125°C (data not shown). These results confirmed the sensitivity of the spinae to high temperature.

The thermogram of the second scan differed from the first one in that the P2 transition disappeared whilst the P1 and P3 transitions remained (Fig. 4, B1). Transmission electron microscopy inspection showed no further visible alteration of the sample compared to that before the second scan; trace amount of the spinae was observed. From the third subsequent scan, only the transition peak 3 was observed. The thermograms remained unchanged for the four subsequent DSC scans (Fig. 4, B1), and the spinae completely disappeared. The samples were transparent and no apparent precipitation was observed. Taken together, the first DSC scan resulted in the disintegration of the spinae structure and the unfolding of the beta-structure, which seems to be connected with the irreversible transition at 98°C. The second DSC completely unfolded polymers with transition temperatures between 50°C and 90°C, and polymers with unknown nature persists the reversible transformation at 123°C.

To gain more information about the nature of the spinae we analyzed these samples with infrared spectro-microscope. The recombined proteinase K and the extracted spine samples subjected to different treatments were loaded on an aluminum mirror, dried by evaporation and analyzed. The reflexion spectra of the proteinase K showed typical spectra of proteinaceous amides with the following vibrations: υN-H at 3282 cm^{-1}, υC=O at 1653 cm^{-1}, δN-H and υC-N at 1548 cm^{-1}. More peaks were observed for the spinae extractions, indicating the heterogeneous components present in the samples (data not shown). Interestingly, we observed spectral differences in the region of 1700–1600 nm (Fig. 4 C). The untreated spinae extraction sample displayed a broad band with a maximum at 1600 nm and a shoulder at 1630 nm (Fig. 4, C, black spectrum). Thermal treatment of the samples resulted in a shift of this peak to 1640 nm whereas it remained at the same position when the samples were digested with the proteinase K (Fig. 4, C, green and blue spectra, respectively). The spectrum of the recombined proteinase K was recorded and shown here as a reference. The maximum of the spectrum was at 1652 nm (Fig. 4, C, red spectrum). This wave number range corresponds to the amide I band and has been reported to be significantly different between native beta-sheet proteins and those in inclusion bodies, thermally induced aggregates or amyloid fibrils[27]. In fact, the amide I maxima in the cross-beta structure of amyloid fibrils generally shift 20–30 nm toward the short wavelength[27]. Therefore, the beta-structure in the spine extractions corresponds better to those of amyloid fibrils than to the beta-sheet structures found in native beta-sheet proteins. Together these biophysical data showed features distinct from those of most native proteins.

Discussion

Bacteria produce various extracellular appendages on their outer surfaces. In addition to the well known flagella, pili, and needles, there are two kinds of appendages from Gram-negative bacteria; prosthecate and nonprosthecate (also called echinuliform) appendages[9]. The prosthecate appendages are extensions of the cell wall containing cytoplasm[28], which include the stalks of *Caulobacter* and the hyphae of *Hyphomicrobium* and *Rhodomicrobium*. Spinae are the representatives of the nonprosthecate appendages. Studies have been carried out with respect to their microscopic structures[15,17,29,30] and the growth conditions favorable for spinae production[18,31,32]. Transmission electron microscopy clearly shows that the spinae extend without apparent connection to the cytoplasm, and are unlikely to be extensions from the cell wall. Our data, obtained in this study, are consistent with the previous reports. In addition, proteolysis analysis revealed that spinae are attached to the cell surface by proteins (Fig. S1, D), and cryo-EM images did not reveal any special structure underneath the spinae (Fig. 2). Growth conditions such as pH, salt concentration and temperature affect the synthesis of the spinae by marine pseudomonad D71[18]. In contrast, the production of the spinae in *C. limicola* strain UdG6038 was not influenced by changes in temperature, pH, salt concentration, or illumination over physiological ranges[11]. However, prolonged sulfide starvation stimulated spinae production in this strain. Similar to the *C. limicola* strain, synthesis of the spinae in *Roseobacter* sp. YSCB strains was unlikely

to be controlled by temperature, oxygen content or pH, but was enhanced by the dilution of the growth media. This appears to be due to changes in salt concentration since addition of NaCl in the diluted media reduced spination. It is unknown how salt concentration influences the production of spinae. These results show that spinae production is regulated by different environmental and physiology parameters depending on the species analyzed.

Spinae are found in Gram-negative bacteria with various physiologies ranging from heterotrophic to phototrophic, both aerobic and anaerobic. Spinae might be omnipresent in aquatic bacteria but only occasionally observed and their synthesis is tightly controlled by environmental parameters and nutrient availability. The Arctic seawater bacterium R7967 and *Roseobacter* sp. DSS-1 that are closely related to *Roseobacter* sp. YSCB isolates, might synthesize the spinae when they are incubated under appropriate conditions. The possible functions of spinae include improving cellular buoyancy, stabilizing capsule structure to retain sulfur colloids, allowing cell-cell contact and signal exchange, aggregation of cells, protection against predation and adhesion to nutrient particles[9–11,16]. To date, none of these hypothetical functions has been experimentally proven. We compared the sedimentation of *Roseobacter* sp. YSCB cells by a method similar to that used for measuring sedimentation rate of red blood cells, and did not find difference between the cells without spinae (grown in normal Marine Broth media) with those with spinae (grown in diluted media). Therefore, the spinae of the *Roseobacter* sp. YSCB strain are unlikely to serve as buoyancy structures to help the cells maintain at a position within the stratified water column. Cryo-EM revealed the absence of the basal body structure underneath the spinae of *Roseobacter* sp. YSCB strain, which excludes a rotary propeller function as the flagella. Consistently, spinae were observed for non-motile bacteria such as *C. limicola*[10,11]. We found that dilution of growth media triggered the spination of *Roseobacter* sp. YSCB strain. Therefore, the spinae might increase cellular surface to improve nutrient binding and uptake. Spinae might have multiple functions depending on ecological niches where the spinae covered cells live.

Bacterial surface appendages are generated by different mechanisms. Flagella, pili, type IV pili and injectisomes are polymerized from proteinaceous subunits via a dedicated protein secretion and assembly apparatus[33–35]. Stalk appendages are extensions of the cell wall and disrupted with lysozyme treatment[36]. Compared to these appendages, the spinae exhibit some distinct features. First, cryo-EM analysis and lysozyme treatment clearly showed that the spinae are not extensions of the cell wall, hence belonging to the family of non-prosthecate appendages. Second, TEM, AFM and cryo-EM inspections showed an unambiguous helical structure of the spinae. Consistently, proteolysis treatment unwound a spine into a proteolysis-resistant filament. These findings allow us proposing the hypothetic spinae assembly mechanism, according to which a filament rotates about an axis, which is accompanied by translation along the axis. Proteins that connect neighboring turns in the helix maintain the helical structure. The distance between the neighboring turns is different according to the analysis method used. The negatively stained TEM images showed that the helix is highly compact whereas relatively large rib spacing was observed for the spinae of the cryo-EM images (Fig. 2, panels Bs versus Cs). Several hypotheses might account for this discrepancy. The uranyl acetate used in negative staining might fill up the gaps between the neighboring turns. Alternatively, the electron density generated from the proteins connecting the neighboring turns is too weak in the cryo-EM analysis. At present, we do not know how hermetic the spinae are. Finally, the thermal treatment ripped the spinae of *Roseobacter* sp. YSCB strain into ribbons. We interpret this observation by suggesting a cooperative rip to change curvature of the helix. The ribbons tend to curl because they consist of ribs with about 6.6° inclination. High-resolution microscopy analysis of the filament ultra-structure might assess this hypothesis.

We have never observed columnar structure directly connected to the cell surfaces. In contrast, the large sides of flares are always linked to the cells and the narrow, distal part is connected to the columnar structure with different length. This observation would suggest that the spine production starts with the flares and then the columnar part. The synthesis of flares should be relatively fast once started or the intermediate product is highly unstable because we have never observed different stage of flare production despite of almost ten-year effort. It is partially because that we can examine the structure only under electron microscopes and the immature structure might be destroyed during the sample preparation.

We attempted to determine the nature of the spinae of *Roseobacter* sp. YSCB strain by various biochemical and biophysical approaches. MALDI-TOF analysis of spinae failed to give any significant peaks in the size range examined (50 000–500 Da). This is not surprising, as it seems unlikely that subunits of such a robust large presumably polymeric structure will be easily extracted and put into the gas phase in the presence of multiple interactions with neighboring subunits. Enzymatic treatment digested the polypeptides present in the spine extracts. However the relationship of these polypeptides to the spine structure is unclear as they are completely digested under conditions where the spinae remain intact. Analysis of the structural protein of the spinae by MS/MS was unfeasible as we are currently unable to obtain soluble peptide fragments for analysis. We found that the spinae are extremely resistant to proteolysis and are relatively thermal stable. The unexpectedly high transition temperature of 98°C observed by DSC has been previously reported for the unfolding transition of large amyloid aggregates[26]. Furthermore the rather low frequency vibration of the amide I band at 1600 cm^{-1} is also characteristic of amyloid like beta sheet structures[27]. Such a structure would also explain the proteinase resistance of the spinae. It thus seems possible that the repetitive helical structure is based on an amyloid like peptide polymerization, though the N:O ratio indicates that the structure is not based uniquely on this. The formation of spinae might thus rely on a polymerization of beta-sheet structures similar to amyloid plaque formation. Taken together, the spinae of *Roseobacter* sp. YSCB strain are distinguished from other bacterial surface appendages, such as flagella, stalks and pili, by both their structure and assembly mechanisms.

Methods

Purification and treatment of the spinae. The *Roseobacter* sp. YSCB isolates were incubated in marine broth M2216 (Difco) at normal or diluted concentration at 28°C with 200 rpm rotary shaking. Cells were harvested by centrifugation at 6000 g for 10 min, washed once with deionized water and resuspended in deionized water. Appendages were sheared by 20 passages of the cellular suspension through 0.8×40 nm needles and harvested in the supernatant fraction after centrifugation at 14 000 g for 10 min. The spinae suspension was either treated directly at 100°C for indicated times, or mixed with Tris-HCl buffer at pH 8 to the final concentration of 20 mM and then treated with various enzymes and DTT. Proteinase K (recombinant PCR grade, Roche Applied Sciences) was used according to manufacturer's instruction. Denaturing, SDS-polyacrylamide gel electrophoresis was performed as previously described[37].

TEM, XEDS and AFM microscopy analyses. Transmission electron microscopic analysis was described previously[38]. The bacteria or purified spinae, absorbed on Formvar-carbon coated grids, were negatively stained with 1% uranyl acetate for 1 min. Examination was performed with a Zeiss EM9 microscope at 80 kV.

Alternatively, samples were examined without fixing nor staining using a transmission electron microscope (JEOL 2100F) equipped with energy dispersive X-ray spectroscopy (XEDS, Jeol) and scanning TEM device.

Atomic Force Microscopy was performed using a Topometrix TMX-2000 Explorer (dry scanner, tapping mode) on specimens adsorbed on freshly cleaved Muscovite V-1 treated with 0.1% uranyl acetate and air-dried.

Cryo-electron microscopy (cryo-EM) and cryo-electron tomography (cryo-ET). Five microliters of purified spinae were deposited onto a glow discharged, C-flatTM holey carbon-coated grid. The excess of the solution was manually blotted, 1 second, with a filter paper. Samples were then quickly frozen into liquid ethane using Leica EM CPC equipment (Leica Microsystems). The grids were placed onto a Gatan 626

cryo-holder, and transferred into the microscope. Sample observations were performed on a Tecnai-G2 LaB6 microscope (FEI Company) operating at 200 kV, at a temperature of about −177°C, and under low dose conditions. Images were recorded on a 2k × 2k FEI Eagle CCD (FEI Company).

Cryo-ET of the spinae were collected at a magnification of 14 500, with the FEI Automated Tomography, Xplore 3D (FEI Company), tilted from −65° to +65° with a 1° step, at a defocus of about −10 µm. Final tomogram is constituted of 131 images with an electron dose per tomogram evaluated at 120 e-/Å2.

Alignment of the tilt series and tomographic reconstructions (calculated by Simultaneous Iterative Reconstruction Technique) were computed with Inspect 3D (FEI Company). Colloidal Gold particles (10 nm) were tracked as fiducial markers to align the stack of tilted images. Voltex volume, segmentation (manually performed) and 3D visualization were carried out with Amira (Visage Imaging GmbH).

Biophysical analyses. *Differential scanning calorimetry (DSC) analysis*. Microcalorimetric measurements were carried out with a high-sensitivity differential scanning VP-DSC microcalorimeter (GE Health Care, Origin Software) with a 0.51 mL cell at heating rates of 60°C/hour between 30 and 125°C. The heating curves were corrected for the baseline obtained by heating the solvent (pure water) alone.

Circular dichroism analysis. CD Spectra were recorded on a J-810 spectropolarimeter (Jasco, Tokyo, Japan). Measurements were recorded between 190 and 300 nm in 10 mm cells at 20°C. Each spectrum is the sum of at least three scans, after baseline subtraction (pure water).

Dynamic light scattering analysis. The measurement of macromolecule sizes was analyzed by dynamic light scattering using a NanoZS (Malvern Instrumenyts Inc., UK). For the experiments, 5 µL of each sample were diluted in 70 µL of pure water. Three records of at least three scans were recorded.

The FT-IR spectro-microscope is composed of the Thermo Nicolet Nexus infrared bench associated with an infrared Thermo Nicolet Continuum microscope. One drop of spinae suspension was dried up by evaporation and examined first under the microscope. The IR spectra of various regions were recorded and analyzed. The analyses were performed at CNRS Service Central d'Analyse in Solaize.

1. Buchan, A., Gonzalez, J. M. & Moran, M. A. Overview of the marine roseobacter lineage. *Appl. Environ. Microbiol* **71**, 5665–5677 (2005).
2. Bruhn, J. B. *et al*. Ecology, inhibitory activity, and morphogenesis of a marine antagonistic bacterium belonging to the *Roseobacter* clade. *Appl. Environ. Microbiol.* **71**, 7263–7270 (2005).
3. Ruiz-Ponte, C., Samain, J. F., Sanchez, J. L. & Nicolas, J. L. The benefit of a *Roseobacter* species on the survival of scallop larvae. *Mar. Biotechnol. (NY)* **1**, 52–59 (1999).
4. Hjelm, M. *et al*. Selection and identification of autochthonous potential probiotic bacteria from turbot larvae (*Scophthalmus maximus*) rearing units. *Syst. Appl. Microbiol.* **27**, 360–371 (2004).
5. Rao, D., Webb, J. S. & Kjelleberg, S. Microbial colonization and competition on the marine alga. *Ulva australis Appl. Environ. Microbiol.* **72**, 5547–5555 (2006).
6. Bruhn, J. B., Gram, L. & Belas, R. Production of antibacterial compounds and biofilm formation by *Roseobacter* species are influenced by culture conditions. *Appl. Environ. Microbiol.* **73**, 442–450 (2007).
7. Slightom, R. N. & Buchan, A. Surface colonization by marine roseobacters: integrating genotype and phenotype. *Appl. Environ. Microbiol.* **75**, 6027–6037 (2009).
8. Moll, G. & Ahrens, R. A new type of fimbriae. *Arch. Mikrobiol.* **70**, 361–368 (1970).
9. McGregor-Shaw, J. B., Easterbrook, K. B. & McBride, R. P. A bacterium with echinuliform (nonprosthecate) appendages. *Int. J. Syst. Bacteriol.* **23**, 267–270 (1973).
10. Brooke, J. S., Thompson, J. B., Beveridge, T. J. & Koval, S. F. Frequency and structure of spinae on *Chlorobium* spp. *Arch. Microbiol.* **157**, 319–322 (1992).
11. Pibernat, I. V. & Abella, C. A. Sulfide pulsing as the controlling factor of spinae production in *Chlorobium limicola* strain UdG 6038. *Arch. Microbiol.* **165**, 272–278 (1996).
12. Lie, T. J., Clawson, M. L., Godchaux, W. & Leadbetter, E. R. Sulfidogenesis from 2-aminoethanesulfonate (taurine) fermentation by a morphologically unusual sulfate-reducing bacterium, *Desulforhopalus singaporensis* sp. nov. *Appl. Environ. Microbiol.* **65**, 3328–3334 (1999).
13. Bowman, J. The Methanotrophs - the families *Methylococcaceae* and *Methylocystaceae*. *Prokaryotes* **5**, 266–289 (2006).
14. Jezberova, J. & Komarkova, J. Morphological transformation in a freshwater *Cyanobium* sp. induced by grazers. *Environ. Microbiol.* **9**, 1858–1862 (2007).
15. Perkins, F. O., Haas, L. W., Phillips, D. E. & Webb, K. L. Ultrastructure of a marine *Synechococcus* possessing spinae. *Can. J. Microbiol.* **27**, 318–329 (1981).
16. Bayer, M. E. & Easterbrook, K. Tubular spinae are long-distance connectors between bacteria. *J. Gen. Microbiol.* **137**, 1081–1086 (1991).
17. Easterbrook, K. B. & Coombs, R. W. Spinin: the subunit protein of bacterial spinae. *Can. J. Microbiol.* **22**, 438–440 (1976).
18. Easterbrook, K. & Sperker, S. Physiological controls of bacterial spinae production in complex media and their value as prediction of spina function. *Can. J. Microbiol.* **28**, 130–136 (1982).
19. Hoyle, B. D. & Easterbrook, K. B. Electrophoretic studies on the cell envelope of a spina-producing marine pseudomonad. *Can. J. Microbiol.* **32**, 901–908 (1986).
20. Gao, J. *et al*. Isolation and characterization of novel marine *Roseobacter* clade members producing unique intracellular chromium-rich aggregates. *Res. Microbiol.* **157**, 714–719 (2006).
21. Brooke, J. S., Koval, S. F. & Beveridge, T. J. Unusually stable spinae from a freshwater *Chlorobium* sp. *Appl. Environ. Microbiol.* **61**, 130–137 (1995).
22. Privalov, P. L. & Khechinashvili, N. N. A thermodynamic approach to the problem of stabilization of globular protein structure: a calorimetric study. *J. Mol. Biol.* **86**, 665–684 (1974).
23. Sturtevant, J. M. Biochemical applications of differential scanning calorimetry. *Ann. Rev. Phys. Chem.* **38**, 463–488 (1987).
24. Privalov, P. L. Stability of proteins: small globular proteins. *Adv. Protein Chem.* **33**, 167–241 (1979).
25. Jelesarov, I. & Bosshard, H. R. Isothermal titration calorimetry and differential scanning calorimetry as complementary tools to investigate the energetics of biomolecular recognition. *J Mol Recognit* **12**, 3–18 (1999).
26. Morel, B., Varela, L. & Conejero-Lara, F. The thermodynamic stability of amyloid fibrils studied by differential scanning calorimetry. *J. Phys. Chem. B* **114**, 4010–4019 (2010).
27. Zandomeneghi, G., Krebs, M. R., McCammon, M. G. & Fandrich, M. FTIR reveals structural differences between native beta-sheet proteins and amyloid fibrils. *Protein Sci.* **13**, 3314–3321 (2004).
28. Staley, J. T. Prosthecomicrobium and *Ancalomicrobium*: new prosthecate freshwater bacteria. *J. Bacteriol.* **95**, 1921–1942 (1968).
29. Easterbrook, K. B., Willison, J. H. & Coombs, R. W. Arrangement of morphological subunits in bacterial spinae. *Can. J. Microbiol.* **22**, 619–629 (1976).
30. Willison, J. H. M., Easterbrook, K. B. & Coombs, R. W. The attachment of bacterial spinae. *Can. J. Microbiol.* **23**, 258–266 (1977).
31. Easterbrook, K. B. & Alexander, S. A. The initiation and growth of bacterial spinae. *Can. J. Microbiol.* **29**, 476–487 (1983).
32. Easterbrook, K. B. Analysis of spinin expression and spina development using phenethyl alcohol. *Can. J. Microbiol.* **33**, 874–878 (1987).
33. Fronzes, R., Remaut, H. & Waksman, G. Architectures and biogenesis of non-flagellar protein appendages in Gram-negative bacteria. *EMBO J.* **27**, 2271–2280 (2008).
34. Macnab, R. M. How bacteria assemble flagella. *Annu. Rev. Microbiol.* **57**, 77–100 (2003).
35. Cornelis, G. R. The type III secretion injectisome. *Nature reviews* **4**, 811–825 (2006).
36. Shapiro, L. Differentiation in the *Caulobacter* cell cycle. *Annu. Rev. Microbiol.* **30**, 377–407 (1976).
37. Santini, C. L. *et al*. A novel sec-independent periplasmic protein translocation pathway in *Escherichia coli*. *EMBO J.* **17**, 101–112 (1998).
38. Pradel, N., Santini, C. L., Bernadac, A., Fukumori, Y. & Wu, L.-F. Biogenesis of actin-like bacterial cytoskeletal filaments destined for positioning prokaryotic magnetic organelles. *PNAS* **103**, 17485–17489 (2006).

Acknowledgements

We thank S. Robert and S. Canaan for advice regarding to lipid analysis, H. Celia for initial cryo-electron microscopy observation, and R. Lebrun for assistance in proteomic analysis. This work was supported by grants from CNRS and CAS to LIA-BioMNSL.

Author contributions

L.-F.W. and A.B. conceived the experiments. A.B., P.B. and C.N. performed TEM, AFM and CET analyses; C.V. carried out DSC, CD and DLS analyses; N.M. for XEDS analysis and J.S. for IR spectroscopy. L.-F.W. and C.-L.S. performed biochemistry analysis, L.-F.W. and T.X. studied spine production and the growth of strain; L.-F.W., C.V. and J.S. wrote the manuscript. All authors reviewed the manuscript.

Additional information

Supplementary information accompanies this paper at http://www.nature.com/scientificreports

Competing financial interests: The authors declare no competing financial interests.

How to cite this article: Bernadac, A. *et al*. Structural properties of the tubular appendage spinae from marine bacterium *Roseobacter* sp. strain YSCB. *Sci. Rep.* **2**, 950; DOI:10.1038/srep00950 (2012).